

PROCEEDINGS OF SPIE

[SPIDigitalLibrary.org/conference-proceedings-of-spie](https://spiedigitallibrary.org/conference-proceedings-of-spie)

GMTNIRS (Giant Magellan Telescope Near-Infrared Spectrograph): structural-mechanical design

Timothy A. Beets, Joseph H. Beno, Moo-Young Chun, Sungho Lee, Chan Park, et al.

Timothy A. Beets, Joseph H. Beno, Moo-Young Chun, Sungho Lee, Chan Park, Marc Rafal, Michael S. Worthington, In-Soo Yuk, "GMTNIRS (Giant Magellan Telescope Near-Infrared Spectrograph): structural-mechanical design," Proc. SPIE 8446, Ground-based and Airborne Instrumentation for Astronomy IV, 844669 (24 September 2012); doi: 10.1117/12.927022

SPIE.

Event: SPIE Astronomical Telescopes + Instrumentation, 2012, Amsterdam, Netherlands

GMTNIRS (Giant Magellan Telescope Near-Infrared Spectrograph): structural-mechanical design

Timothy A. Beets*^a, Joseph H. Beno^a, Moo-Young Chun^b, Sungho Lee^b, Chan Park^b, Marc Rafal^c,
Michael S. Worthington^a, In-Soo Yuk^b,

^aCenter for Electromechanics, University of Texas, 10100 Burnet Rd., EME 133, Austin, TX 78758;

^bKorea Astronomy and Space Science Institute, 776, Daedeokdae-ro, Yuseong-gu, Daejeon,
Republic of Korea 305-348

^cMcDonald Observatory, College of Natural Sciences, University of Texas, 2515 Speedway, Stop
C1402, Austin, TX 78712

ABSTRACT

A near-infrared spectrograph (NIRS) has been designed and proposed for utilization as a first-light instrument on the Giant Magellan Telescope (GMT). GMTNIRS includes modular JHK, LM spectrograph units mounted to two sides of a cryogenic optical bench. The optical bench and surrounding, protective radiation (thermal) shield are containerized within a rigid cryostat vessel, which mounts to the GMT instrument platform. A support structure on the secondary side of the optical bench provides multi-dimensional stiffness to the optical bench, to prevent excessive displacements of the optical components during tracking of the telescope. Extensive mechanical simulation and optimization was utilized to arrive at synergistic designs of the optical bench, support structure, cryostat, and thermal isolation system. Additionally, detailed steady-state and transient thermal analyses were conducted to optimize and verify the mechanical designs to maximize thermal efficiency and to size cryogenic coolers and conductors. This paper explains the mechanical and thermal design points stemming from optical component placement and mounting and structural and thermal characteristics needed to achieve instrument science requirements. The thermal and mechanical simulations will be described and the data will be summarized. Sufficient details of the analyses and data will be provided to validate the design decisions.

Keywords: near-infrared, spectrograph, GMT, CEM, KASI, cryostat, structural, simulation

1. INTRODUCTION

GMTNIRS (Giant Magellan Telescope Near-Infrared Spectrograph) conceptual design has been finalized and was submitted for candidacy as one of the three first light instruments for the GMT. This design effort was carried out by numerous organizations including the University of Texas at Austin, the Korea Astronomy and Space Science Institute, and Kyung Hee University. GMTNIRS is a cryogenic instrument located on the GMT rotating instrument platform and is fed by the GMT facility adaptive optics system. The instrument observes the entire spectrum transmitted by the Earth's atmosphere between 1.12 and 5.3 μm and is capable of a 3-4 magnitude improvement in sensitivity and a factor 50-200 improvement in instantaneous wavelength coverage over existing high spectral resolution instruments.

1.1 Design emphasis

The design emphasis for GMTNIRS was placed on obtaining high sensitivity, resolution, and versatility at modest cost and low risk. This lofty design goal was realized by 1) utilizing the unique traits of GMT, namely the large collecting area and the adaptive secondary, 2) technological improvements in low-noise, high QE detectors and high-efficiency echelle and cross-disperser gratings, and 3) providing simultaneous coverage of the entire target wavelength range at high resolution in a single exposure^{1,2}.

1.2 GMTNIRS design overview

As shown in Figure 1, GMTNIRS comprises five individual spectrographs for the J, H, K, L, and M bands, which all share a common slit.

*t.beets@cem.utexas.edu; phone 1 512 232-4285; fax 1 512 471-0781; www.utexas.edu/research/cem/

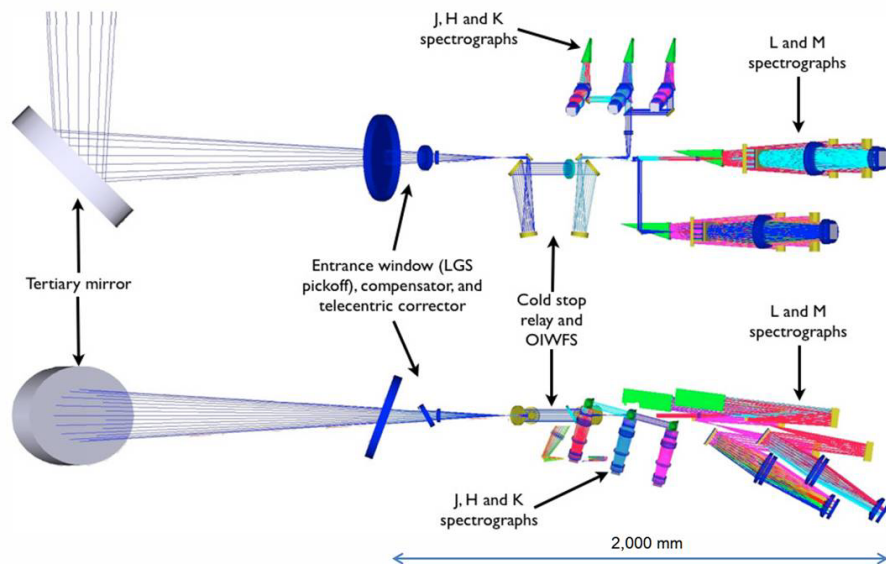


Figure 1. Overview of the GMTNIRS optical design. The GMT tertiary mirror is shown along with the cold pupil relay and the 5 individual spectrograph channels.

The full coverage of the spectrographs means GMTNIRS can operate with a single cryogenic moving part, the rotating pupil wheel, with no moving parts after the entrance slit of the spectrograph. Accordingly, solid mounts for optical components provide for a much more stable instrument during gravity-variable operation³.

GMTNIRS sits on the GMT instrument platform, at a focus provided by the folded tertiary mirror. The entrance slit, which is common to all spectrograph channels, follows a cold stop and relay optics. All five spectrographs are modular, where the J, H, and K designs are similar to each other, but distinct from the L and M channel design.

1.3 Instrument requirements

As GMTNIRS will reside on the GMT instrument platform (IP), and will probably be only one of multiple instruments installed on the platform, some considerations stem from telescope-specific physical requirements. The first is regarding the available instrument volumetric envelope. The right-hand image of Figure 2 shows GMTNIRS residing in one of four pie-shaped instrument envelopes available on the IP. Additionally, there are preferred buffer zones of 1m between adjacent instrument envelopes to allow maintenance access to the instruments. The instrument height is also limited by the overhead allowance of 1.8m available on the IP. Finally, the instrument system mass is limited by deflection limits IP and drive considerations of the telescope to no more than 2 tons.

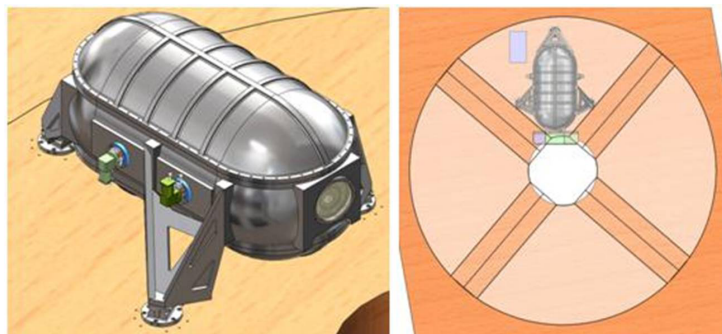


Figure 2. GMTNIRS on the GMT instrument platform. Right image shows GMTNIRS as it resides in a single instrument envelope. 1m Buffer zones are shown between adjacent envelopes.

Additional requirements stem from the optical alignment study performed during concept design of GMTNIRS⁴. Regarding the optical bench, the absolute displacement by flexure must be held below +/-50µm, while the relative displacement over a one hour observation must be maintained below +/-10µm. Thermal efficiency and stability of the instrument are also subject to limitation. Thermal design of the instrument requires reaching steady state temperatures of 70 +/-4 °K for optical bench, optical elements, channel housings and shields, 70 ±10°K for the radiation shield, 65°K for the J, H, and K detectors, and 37°K for the L and M detectors (with an operating temperature range between -10°C (263°K) to 25°C (~300°K)). Further, a temperature gradient less than ±4°K must be maintained over a typical scale of 100mm between components to keep the resulting displacement by differential thermal contraction smaller than the 10µm manufacturing tolerance.

2. MECHANICAL DESIGN

The proposed GMTNIRS instrument is housed within an aluminum cryostat mounted to the GMT Instrument Platform. The cryostat is designed to house and rigidly support an aluminum optical bench and all hardware pertaining to instrumentation of the optical components within the cryostat, as well as cold heads, vacuum lines, and additional instrumentation outside the cryostat. Figure 2 shows the GMTNIRS cryostat mounted to the GMT Instrument Platform, along with the external wave front sensor and electronics box (in the right hand image). The footprint and envelope, as well as the 1m buffer zones (shown as 2 adjacent 0.5m buffers) for the instrument are illustrated as well. As shown, the GMTNIRS instrument fits well within the GMTO specified envelope and is quite compact for its capabilities. Figure 3 and Table1 lists several of the general physical parameters of the instrument.

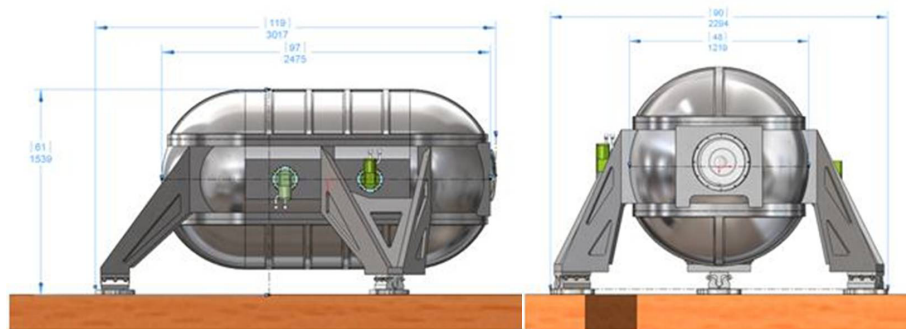


Figure 3. Side and front views of instrument showing overall and dewar dimensions (dimensions are in mm with inches shown in brackets).

Table 1. General physical specifications of instrument.

<u>Specification</u>	<u>Value</u>	<u>Unit</u>
Cryostat mass	971	kg
Optical bench mass	370	kg
Total system mass	1639	kg
Cryostat length	2.9	m
Cryostat width	2.2	m
Cryostat height	1.84	m

2.1 Cryostat

The sealed cryostat has multiple entry points, the primary entry being the optical input window at one end. Other entry points allow for pass-through of instrumentation, cold heads, etc. As shown in Figure 4, the optical bench is suspended within the cryostat by a thermal isolation system and is protected from thermal radiation via a high-reflectivity shield.

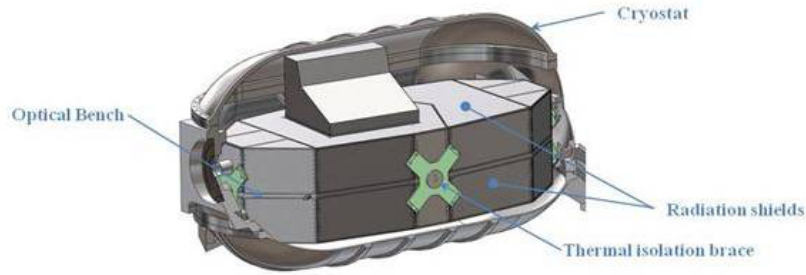


Figure 4. Cut-away view of the optical bench with radiation shield in place, suspended within the cryostat.

The GMTNIRS cryostat is a typical vacuum vessel design with a cylindrical main body and 1:1 hemispherical heads. The material chosen for the cryostat is aluminum 6061-T6, which has been utilized effectively in many previous instruments. Figure 5 shows the dimensions of the revolved baseline body of the cryostat. As shown, the length is 2.5 m, the radius is 0.63 meters (1.26 m total width) and the wall thickness is 9.53 mm (0.375 in.).

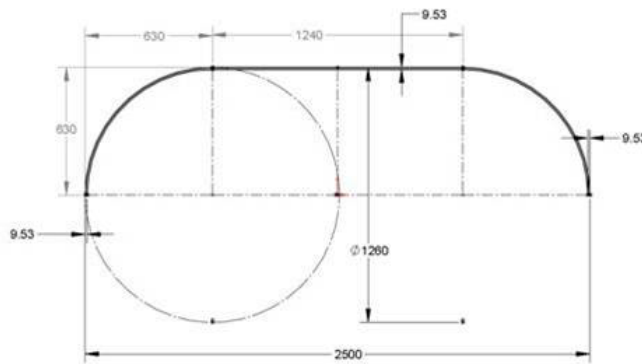


Figure 5. Dimensions (mm) of base revolve feature of cryostat.

The cryostat is split on two horizontal planes, one above and one below the horizontal mid-plane of the cryostat, dividing the vessel into a midsection and two hatches. Illustrated in Figure 6, the cryostat maintains an interior cylindrical cross-section of diameter 1.24 m with the exception of a slight vertical elongation to provide thickened attachment rims for the midsection and hatch components. The split lines (i.e., hatch interface planes) are 0.30 m above and below the centerline. Accordingly, the height of the midsection is 0.60 m.

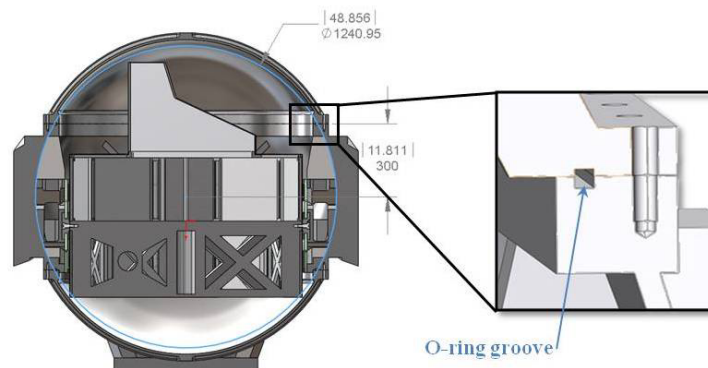


Figure 6. Cross-section of assembled cryostat with detail of hatch o-ring groove.

The hatches are vacuum sealed to the cryostat midsection with o-rings and are secured with bolts peripherally-spaced about the rims of the hatches and midsection. As shown in the enlarged image of Figure 6, the o-ring grooves are formed by partial depth grooves in both mating rim sections. This arrangement prevents scratching of the o-ring faces during handling of the cryostat components⁵. The attachment bolts pass through the hatch rims and thread into blind

holes in the midsection rims. Threaded inserts may also be used to prevent damage to threads from repeated assembly and disassembly of the cryostat. Alignment pins (not shown) are utilized to facilitate proper alignment of the hatches with the midsection and to add lateral stiffness to the hatch/midsection connections.

Shown in Figure 7, the midsection of the cryostat is the structural heart of the instrument. It provides mounting infrastructure for the optical bench (via the thermal isolation system), the support legs which attach to the Instrument Platform, the input window, and mounting and pass-through features for all instrumentation and auxiliary equipment (e.g., cold heads). Accordingly, the hatches are not required to possess any additional auxiliary interface features and can be easily removed or installed without adding significant difficulty to the cryostat assembly process.



Figure 7. Optical bench suspended in cryostat midsection and exploded view of cryostat hatches.

The primary purpose of the cryostat midsection is to act as a rigid mechanical link between the optical bench and the Instrument Platform. Accordingly, the legs and anchor points (to the Instrument Platform) of the midsection are of the utmost significance. A 3-point leg and anchor system was adopted and refined for the cryostat attachment method. Figure 8 shows the dimensional footprint and anchor points of the legs. The legs are angularly spaced about the cryostat (i.e., optical bench) center point. The forward legs are of equal radii (1.1 m) and each is swept forward 115° from center, while the rearward leg is positioned 1.6 m from the center along the centerline of the cryostat.

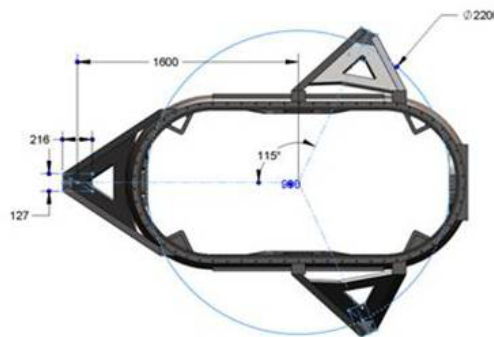


Figure 8. Midsection footprint and anchor point positions.

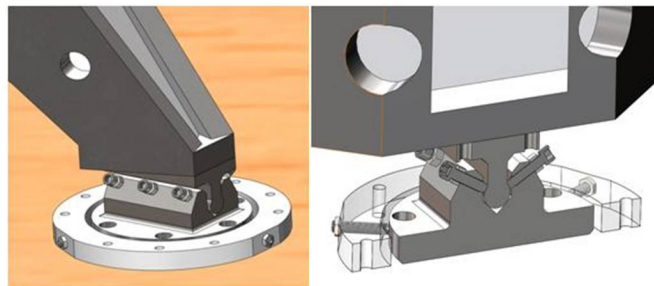


Figure 9. Adjustable, kinematic anchor points.

Figure 9 illustrates the components that anchor the cryostat legs to the Instrument Platform. Essentially, the three legs present a 3-point, cylinder-in-groove type kinematic mount for the cryostat. A cylindrical linear bearing segment (e.g., Thomson Linear) is mounted to the bottom of each leg. Each cylindrical bearing segment is seated into a corresponding V-block module that is connected via bolts to the Instrument Platform. The axes of the cylindrical bearings and V-blocks are aligned toward the center of the cryostat (i.e., optical bench), as in a typical kinematic-style mount. The V-block modules include a series of six retaining bolts to seat the cylindrical bearings into secure engagement with the groove and prevent lift-off during instrument orientation changes. An alignment ring is located around the periphery of each V-block module. The alignment ring is secured to the Instrument Platform with a series of bolts. Three (3) adjustment bolts within the alignment ring may be used, in conjunction with shims, to re-orient the V-block modules to allow for alignment of the instrument optical axis to the tertiary mirror.

It is assumed that the V-block modules will be initially aligned (with pre-drilled holes in the Instrument Platform) via a high-precision positioning system, such as a laser tracking system. Once the instrument is installed, adjustments to the optical axis of the cryostat may be executed by re-orientating the V-block modules.

The cryostat optical input window is shown in Figure 10. The input side cryostat (midsection) head has a seat support that is angled (about a vertical axis) to orient the window relative to the optical bench input light path and the AO system. The optical input axis is offset 10° from the cryostat centerline. The input window is mounted to the seat support, which is oriented an additional 10° from the centerline. Accordingly, the input optical path intersects the input lens at a 20° offset, providing a further 20° offset for the external wave front sensor optical pick-up.

The seat support is machined with a pair of concentric o-ring grooves to form a vacuum seal between the lens and the cryostat. The pair of concentric rings distributes the reactant force of the vacuum pressure across a broader area of the window, thereby reducing deflection of the window. A retaining ring, bolted to the cryostat, maintains a preload of the lens against the o-rings via a wave spring. The wave spring (Smalley SSB-1378) chosen for the concept design is capable of providing 961N at working height (3mm). This height can be optimized to provide a specific preload force on the lens. The retaining ring includes three equally-spaced leaf springs to center the lens and allow for thermal expansion variations between the cryostat and lens⁵.

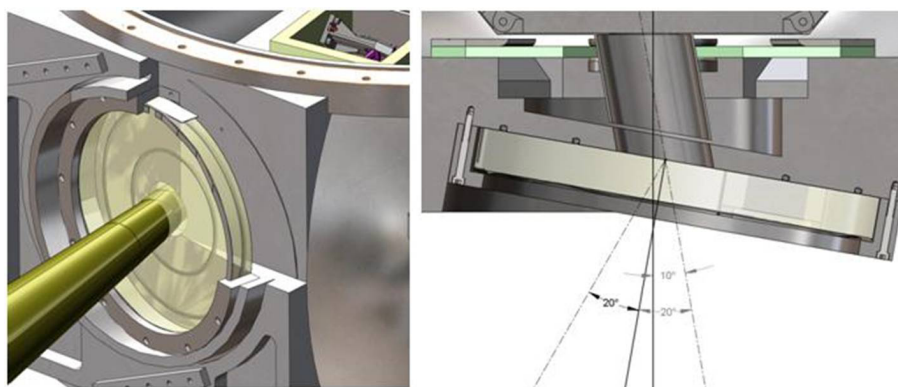


Figure 10. The GMTNIRS cryostat optical input window. Circumferentially-spaced leaf springs keep the lens centered during thermal contraction/growth while a wave spring maintains axial preload on the o-rings to maintain the vacuum seal.

2.2 Primary optical bench

The main GMTNIRS optical bench is a 3-component modular bench. Shown in Figure 11, the uppermost component is the primary optical bench. This bench serves as the mounting platform for the AO, slit, WFS, and L/M band optical support hardware. One unique feature of GMTNIRS is that both sides of the primary optical bench are utilized for hardware mounting.

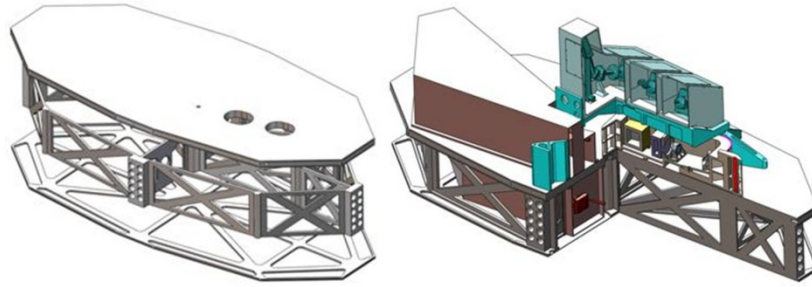


Figure 11. Details of modular optical bench. Left-hand image shows three-piece modular assembly and right-hand image shows installation arrangement of main optical subcomponents.

All modules are fabricated from aluminum 6061-T6 material. The primary optical bench is a 40mm-thick faceted ellipsoidal plate. The underside of the primary bench is machined with multiple pockets to reduce mass. Additionally, the edges of the primary bench have threaded holes that interact with the thermal isolation system discussed below.

The second modular component of the main bench is a truss-type support structure (also referred to as space-frame) attached to the underside of the primary optical bench. The use of such truss supports was effectively utilized in the SPIFFI instrument. The support structure is carefully designed to provide rigidity and stiffness to the primary optical bench without adding significant mass to the system. In addition, the structure does not interfere with the optical components mounted to the underside of the primary bench. The support structure will be fabricated in sections, which will be joined by welding. The welded structure will be stress-relieved (thermal and vibratory) and re-aged to the T6 condition.

The third module of the optical bench is a secondary plate mounted to the bottom of the support structure. The secondary plate provides the support structure with lateral stiffness, increasing the rigidity of the support structure. Further, the secondary plate serves as a unitary bottom cover for the radiation shield. The top of the secondary plate is machined with multiple pockets to reduce mass. The modules of the main bench are interconnected with dowel pins, for alignment and shear strength, and with bolted connections.



Figure 12. Auxiliary optical bench and J, K, H channel housing details.

2.3 Auxiliary optical bench

One other unique feature of the GMTNIRS optical bench is the use of a raised (relative to the main optical bench) auxiliary bench to mount the J, K, and H channel housings. Shown in Figure 12, the auxiliary bench is mounted to the top of the optical bench on rigid risers and provides a platform to support the J, K, H channel housings.

Each of the J, K, H channel housings has a main support plate that is oriented normal (i.e., upright) relative to the primary optical bench. This main support plate is the primary mounting and support structure for the corresponding J, K, or H channel optical components. The backside of each support plate is pocketed to reduce mass. The walls of the channel boxes are integral (as in machined from the same piece of billet material—6061-T6) with the support plate. A separate light shield (i.e., cover), which doubles as a stiffener is connected via bolts to the open side of the housing. Various removable plates will be included that will allow access to optical components within each box, but will keep the boxes light-tight when installed. As shown in the far right image of Figure 12, each housing includes three mounting pads (on the bottom of the housing) that contact the auxiliary optical bench.

2.4 Thermal isolation system

The thermal isolation system consists of four X-brace supports positioned at opposing longitudinal and lateral ends of the optical bench, as shown in Figure 13. This orientation dictates that the optical bench geometric center point serves as a static reference point for positioning the optical components on the bench and as a datum during manufacture of the bench.

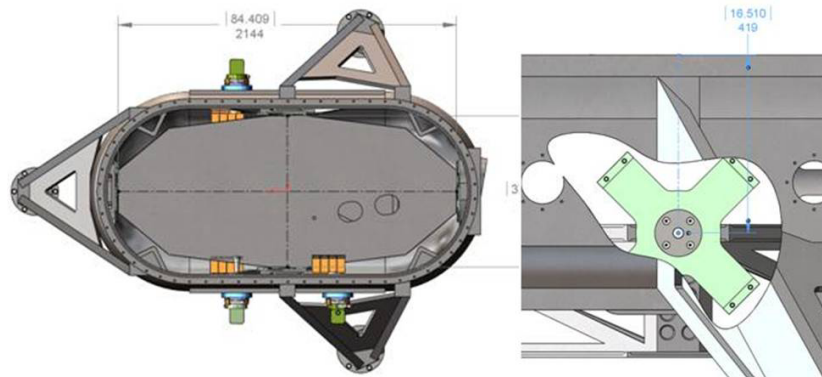


Figure 13. Orientation and alignment of thermal isolation system supports.

Figure 14 shows details of the X-brace supports. The primary component of each brace is an X-shaped member constructed of G10CR (cryogenic-grade GFRP) plate (9.525mm [0.375"] thick). This material was chosen due to its inherent low thermal conductivity in order to thermally isolate the optical bench⁶. Additionally, the material itself, as well as the manner and orientation of the components fabricated from the material can be tailored to provide directionally-based rigidity or flexibility⁷. This trait allowed a design to be completed that provides sufficient flexibility in the directions of thermal contraction of the optical bench, while providing sufficient system rigidity to limit displacement of the bench (i.e., optical train) during rotations of the Instrument Platform. The right-hand image of Figure 14 illustrates the ply directions of the glass fiber weave within the G10CR material.

The ends of the arms of the G10CR members are fastened to cryostat interior mounting features with bolts. Stainless steel backing plates prevent excessive stress concentrations at the fastener interfaces with the G10 material. A stainless steel support member protrudes through the center of the G10 brace and serves a number of functions: First, it provides a solid, direct interface to the optical bench. The support member also has a flange which, along with a backing member, sandwich the G10 plate to provide a strong connection with a large bearing area on the G10 material. A series of bolts and pins, as well as epoxy, connect (and bond) the support member, backing member, and the G10 plate. A precision shoulder bolt, made of the same stainless material as the bearing member (to match CTE effects), passes through the support member and engages a threaded hole in the edge of the primary optical bench. A set screw is utilized to lock the shoulder bolt and prevent incidental back-out of the screw threads during handling and thermal cycling.

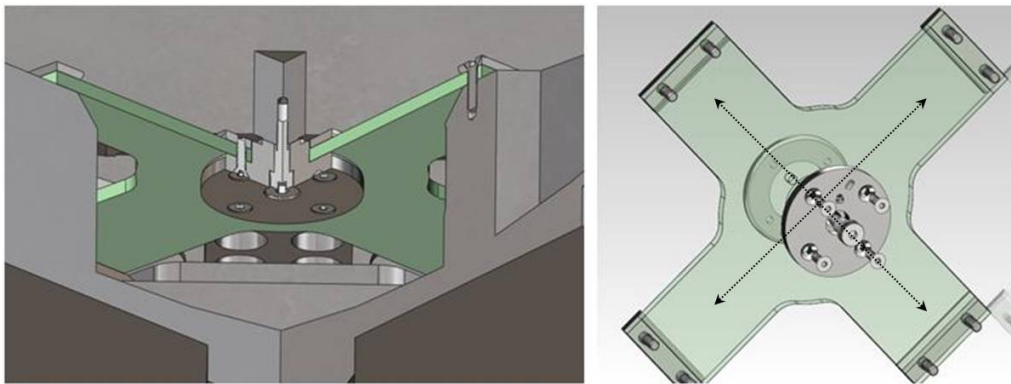


Figure 14. Construction and attachment details of G10CR cross braces of thermal isolation system.

2.5 Radiation shield

A cover is required to shield components on the optical bench from incident light and radiation from the cryostat walls. For the top half of the bench, this radiation shield is comprised of a support structure and sheet metal panels (perimeter and top panels), all fabricated from 1100 series aluminum. The support structure has four types of supports as shown in Figure 15: perimeter supports, internal supports, cross members, and a JHK bucket support. The perimeter supports are located at each corner of the faceted optical bench. The supports have recessed steps which, combined with scalloped pockets in the top and bottom edges of the primary optical bench, provide pockets for attachment of the sheet metal perimeter panels. Attaching the panels in these recessed pockets, as shown in Figure 16, creates a treacherous path for incoming light and radiation. The internal supports and cross members make up the interior support structure. The internal supports serve to support the cross members upon which the top panels lie. The cross members have top rib features that create pockets for the top panels to lie in. Each panel is attached with a series of threaded fasteners and is easily removed to allow access to the optical components should maintenance be required. The protruding section of the J, H, and K modules is covered by a welded sheet metal box referred to as the JHK bucket. This box attaches to the JHK supports located around the perimeter of the JHK modules. In order to minimize radiation, exterior surfaces of both the panels and the supports are polished and interior surfaces are painted black.

The lower radiation shield attaches to the primary optical bench and the optical bench base plate. Vertical supports similar to those used on the top radiation shield extend between the primary optical bench bottom surface and the base plate. Like the upper radiation shield, the perimeter panels are flat sheets of 1100 series aluminum and all exterior surfaces are polished while the interior surfaces are painted black. The perimeter panels attach along their top and bottom edges to the faceted faces of the optical bench and its support structure. Due to the symmetric nature of the radiation shield, for each side and for the top and bottom radiation shields, there are only 4 distinct perimeter panel geometries that will need to be fabricated. The bottom surface of the bottom plate of the support structure is highly polished and acts as the radiation shield for the bottom surface.

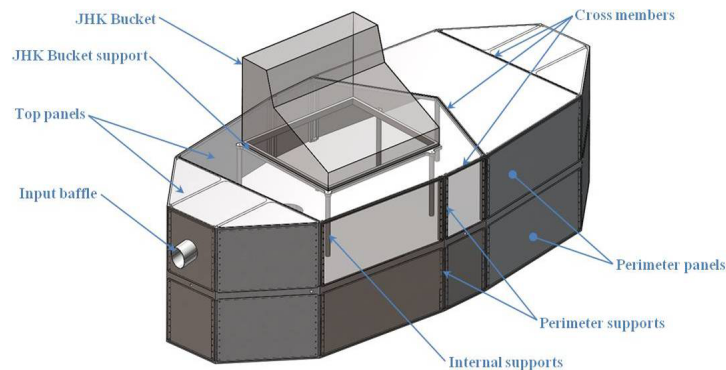


Figure 15. Upper and lower radiation shields installed on optical bench.

As shown in Figure 16, the front panel of the upper radiation shield includes an opening for instrument light passage and a cylindrical baffle to shield this path from radiation between the cryostat interior and the radiation shield. The baffle is attached to the front panel of the radiation shield and extends up to the rear of the input window support of the cryostat. A small gap (refer to Figure 10) is left between the window support and the baffle to prevent heat conduction and allow for relative thermal displacements.

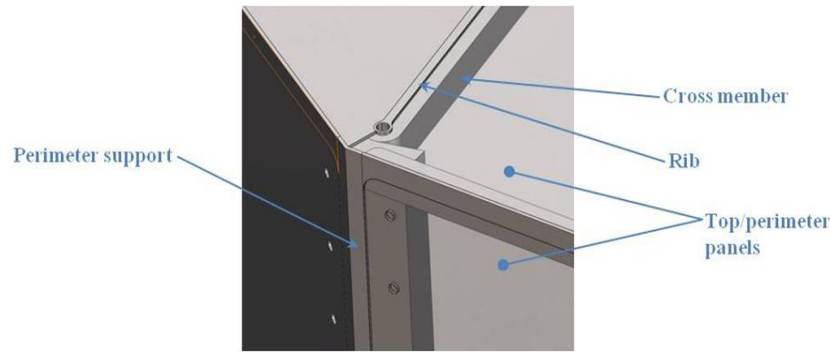


Figure 16. Recessed pockets to prevent light leakage through radiation shield.

2.6 Optical bench layout

The optical train mounts to the optical bench in seven sections, as labeled in Figure 17. Mounting the optics onto separate, stiff housings allows the majority of tight tolerance alignments to be performed on a smaller scale. These housings, machined from 6061-T6 aluminum, can then be cooled to operating temperature independently in a test dewar to further refine the alignment. Upon assembly onto the optical bench, final alignment is achieved by shimming the entire housing, preserving the internal alignments.

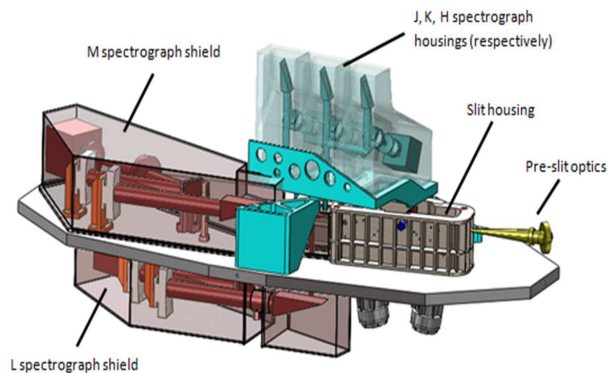


Figure 17. Optical bench (with support structure hidden for clarity) and major subcomponents labeled.

The pre-slit optics consists of a corrector lens for the angled entrance window (LGS pickoff mirror) and a telecentric corrector. The light then enters the slit housing which includes the telescope focal plane, pupil rotator assembly, cold stop, OIWFS and the slit. Mounting both the slit housing and OIWFS to a common, stiff structure ensures control of relative deflection between components during telescope rotations. Two relay mirrors are located on the bottom side of the optical bench. Both the slit housing and the optical bench have cutouts allowing the light path to pass through. The relay mirrors are enclosed in a structure that fastens directly to the slit housing.

After the slit, light is divided into the five bands through a series of dichroic mirrors. The first dichroic separates the JHK bands and collectively directs the light vertically upwards from the surface of the optical bench. The light enters the K housing where two additional dichroic mirrors separate the J and H bands into nearly identical housings. All three housings provide access panels to critical elements for final alignment and are supported on a common subplate. The housings also provide stiffness to prevent excessive deflection throughout the telescope's range of motion.

The L band is then separated from the M band via another dichroic which directs light through the optical bench to the bottom side. Both L and M bands, identical in terms of optical components, are housed in thin-walled, light-tight shields. All optical components fasten directly to the optical bench.

2.7 Pupil rotator

The GMTNIRS instrument has only one internal (cold) moving component—the pupil rotator. This mechanism was designed based on previous instruments: MOSFIRE⁸, OSIRIS, and NIRSPEC⁹. The pupil rotator assembly, Figure 18,

consists of three major parts: the worm drive bearing assembly, mount, and pupil plate. The worm drive assembly is driven by a stepper-motor rated for cryogenic use. The stepper-motor allows the spectrograph's software to count the number of motor steps and thereby track the position of the pupil. Positional sensors are mounted at discrete positions on the worm gear to provide reference points for position tracking. The pupil plate is a separate machined plate that will mount onto the face of the worm gear. Accordingly, the pupil plate may be easily replaced should a need ever arise for a smaller (or larger) pupil diameter. The mechanism mount positions the pupil rotator assembly in the optical path. Slots are used instead of holes to allow the installer to tweak the position of the pupil when mounting the instrument.

The bearing, the worm, the drive shaft, and the pupil plate are constructed of stainless steel. Thermal analyses were performed to assure the induced thermal stress caused by the different thermal expansion rates of steel and aluminum will not compromise the functions of the parts. The mount and the worm drive housing are made of the same material as the optical bench, 6061-T6 aluminum, to match the thermal contraction rate of the bench.

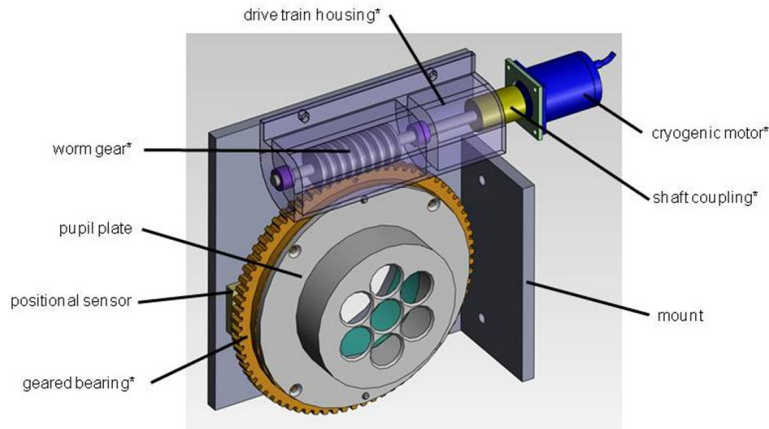


Figure 18. The GMTNIRS pupil rotator mechanism. Labels with asterisks (*) indicate components of custom worm drive assembly.

3. ANALYSES

3.1 Vacuum

Operation of the GMTNIRS instrument requires a vacuum be pulled on the cryostat interior to increase thermal efficiency. An analysis was performed to verify the integrity of the cryostat under hard vacuum (1×10^{-7} torr). Figure 19 shows a plot of the results from this simulation. Maximum stress on the cryostat is 59.3 MPa, which corresponds to a safety factor of 4.3.

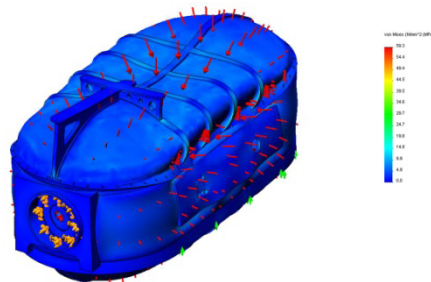


Figure 19. Stress (vM) analysis results of vacuum pressure on cryostat. Deformation is exaggerated for clarity.

3.2 Thermal supports (structural)

A structural verification study was performed on the thermal isolation system braces. Specifically, the supports were analyzed to determine if the G10CR X-braces experienced excessive stresses due to the thermal contraction of the optical bench. As shown in Figure 20, maximum stress in the G10 material is limited to 77 MPa on the surface at the interface of the bearing support. This stress is well under the material's peak limit and preserves a safety factor of 3.9.

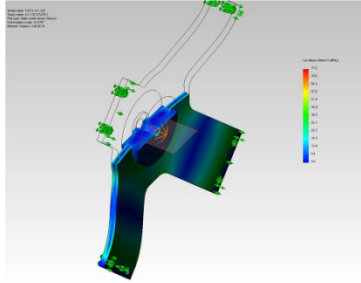


Figure 20. Stress (vM) results plot on G10CR thermal isolation system brace. Deformation exaggerated for clarity.

3.3 Optical bench displacement

Extensive structural analyses were performed to verify satisfactory performance of the optical bench and optical component support elements. These analyses were performed as static studies with a gravity vector varying in 15 degree increments in altitude and azimuth. Figure 21 shows the plot of the results of a displacement simulation with the gravity vector oriented normal to the optical bench top (primary) surface.

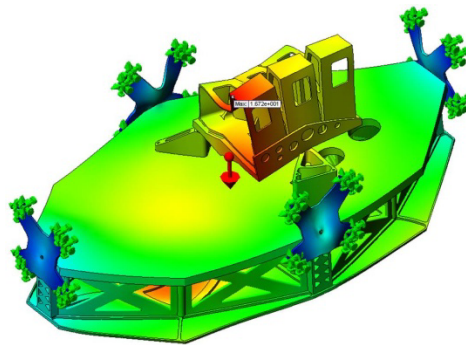


Figure 21. Displacement (μm) results plot of primary and auxiliary optical benches with gravity oriented normal to bench surface. Displacement magnitude is indicated in red and is exaggerated for illustration. Maximum displacement shown in $16.7\mu\text{m}$ at the outer edge of the H spectrograph subplate, well away from the optical component mounts and accounted for with initial alignment of GMTNIRS optical train.

Figure 22 shows the location of simulation sensor nodes positioned on the optical bench primary surface and on the J, K, H spectrograph subplates at optimal optical mount locations. The displacements resulting from a gravity vector normal to the optical bench surface (shown in the left hand image of Figure 22) are accounted for and corrected with the initial instrument alignment procedure.

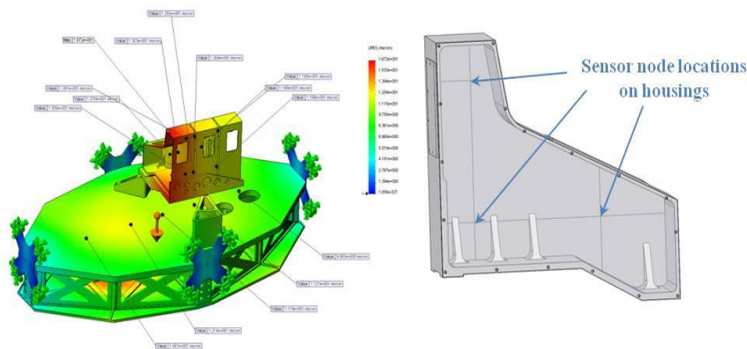


Figure 22. Locations of simulation sensor nodes on optical bench and J, K, H housings (subplates). Left hand image shows maximum displacement plot (undeformed). Maximum displacement (shown in red) at H subplate sensor is $13\mu\text{m}$, corrected during initial instrument alignment.

Table 2 summarizes the results the displacement study. The gravity orientation relative to the optical bench is described by “0-0” with the optical bench in a horizontal orientation (gravity normal to optical bench), “15-15” with the optical

bench tilted at 15° from horizontal and rotated 15° about the IP rotational axis, and so on. The relative movements between these incremental positions are indicated by “0-0/15-15” and so on. As pointed out in Figure 22, five sensor nodes were placed along the longitudinal axis of the optical bench and three nodes were placed on each J, H, K housing (in locations corresponding to optical component mount hardware). These nodes were monitored for displacement changes between incremental instrument re-orientations. As shown, no incremental move imparts a displacement greater than 8.47 microns.

Table 2. Displacement (μm) between gravity orientations at various nodes on optical bench and JHK subplates.

		3D Relative Displacements		
		0-0/15-15	15-15/30-30	30-30/60-60
Optical Bench		-0.24	-0.52	-1.07
		0	-0.15	-0.82
		-0.12	-0.45	-1.31
		-0.06	-0.25	-1.00
		-0.18	-0.58	-1.45
H		-7.34	-8.47	-2.93
		-3.66	-3.67	-1.18
		-1.04	-2.72	-2.90
J		-2.87	-6.14	-3.16
		-0.15	-1.77	-2.56
		-0.86	-2.22	-2.14
K		-0.78	-4.97	-2.48
		-0.85	-1.46	-1.20
		-0.12	-1.69	-2.01

3.4 Thermal analyses

A series of thermal analyses were performed for the entire instrument. Both static and transient analyses were performed to establish the final temperature distribution and the cooling time required to achieve operating temperature. The primary variables in achieving the desired thermal response are adjusting the cooling capacity and cold strap sizes. The desired thermal goals are:

1. Operate in the specified ambient temperature range of -10°C (263°K) to 25°C (~300°K)
2. Achieve steady state temperatures of:
 - a. 70 +0/-4 °K for optical bench, optical elements, channel housings and shields
 - b. 70 ±10°K for radiation shield
 - c. 65°K for JHK detectors (not accounted for in these analyses)
 - d. 37°K for LM detectors (not accounted for in these analyses)
3. Achieve temperature gradient less than ±4°K over a typical scale of 100mm between components to keep the resulting displacement by differential thermal contraction smaller than the 10μm manufacturing tolerance

The following list details the boundary conditions of both thermal analyses:

- Cryogenic properties for thermal conductivity and specific heat are used for 6061-T6 Al and oxygen free high conductivity (OFHC) copper
- Constant temperature equal to the ambient temperature applied to inner surface of cryostat
- Constant temperature applied to all 3 refrigerator cold heads equal to the equilibrium operating point per the manufacturer power curves (varies depending on ambient temperature)

- Heat power (absorption) versus temperature curves for all three cold heads per the manufacturer
 - The curves did not supply power data up to 300°K; the maximum power provided (at 115°K for the M1050 refrigerator and 90°K for the M350) was assumed to remain constant at all higher temperatures providing a conservative estimate
- Radiation between interior surfaces of cryostat and all exterior surfaces of the radiation shield; emissivity = 0.05 (polished exterior and painted black interior of all radiation shield components)
- Current analysis neglects radiation through entrance window, conduction through G10 supports and heat load from pupil rotator motor (each calculated to contribute less than 2% of total heat transfer) and assumes no thermal resistance between parts

The results of the static analysis, Table 3, show that the entire optical bench and all of its major subcomponents achieve a final temperature less than the required 70°K for all ambient conditions. Referencing goal 2a from the previous list, while all components except for the optical bench meet the required 4° temperature distribution tolerance, the overall temperatures are significantly cooler than 70°K. Several options can be explored in the detail design phase for addressing this issue: evaluate optical performance at these cooler temperatures to determine if performance is compromised at these cooler temperatures; reduce the cooling capacity of at least one, if not both, M1050 refrigerators; add external heaters in key locations to raise temperatures in a controlled manner.

These issues are also applicable for the radiation shield. The 25°C ambient temperature case shows that the temperature distribution across the radiation shield exceeds the 10° tolerance (goal 2b). Likewise, at cooler ambient temperatures the radiation shield temperature range is cooler than originally desired. Subsequent analysis is needed to determine if there are any negative consequences with the cooler temperatures.

Table 3. Static temperatures of major subcomponents for different ambient conditions.

Component Temps. (degK)	25°C Ambient			-10°C Ambient		
	Max	Min	Delta	Max	Min	Delta
Rad. Shield	68.5	55.6	12.9	53.9	45.8	8.1
Optical bench surface	63.2	56.4	6.8	50.7	46.3	4.4
Slit housing	62.2	60.7	1.5	50.1	49.2	0.9
M shield	62.6	60.2	2.4	50.6	49.1	1.5
L shield	62.3	60.2	2.1	50.4	48.9	1.5
JHK subplate	62.6	58.8	3.8	50.4	48.1	2.3
J housing	61.1	61.0	0.1	49.5	49.5	0.0
H housing	61.8	61.2	0.6	49.9	49.6	0.3
K housing	61.4	60.9	0.5	49.7	49.4	0.3

Figure 23 is a plot showing the temperature distribution across the optical bench and subcomponents with 25°C ambient conditions. Modifying the cold strap routing from the cold heads to the optical bench will provide a more even temperature distribution. With the current cold strap routing, all components meets the required 4°/100mm temperature gradient (goal 3) as shown in Figure 24.

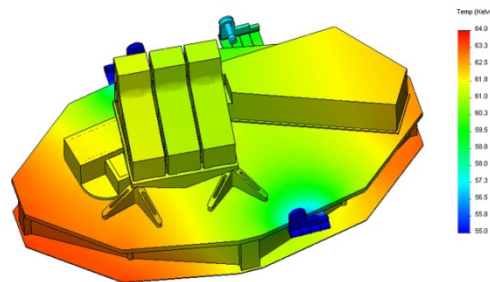


Figure 23. Steady-state temperature distribution of the optical bench and major subcomponents with 25°C ambient temperature.

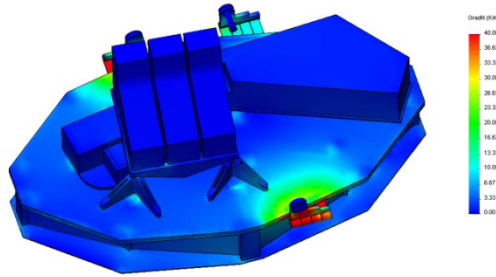


Figure 24. Temperature gradient across the optical bench and major subcomponents with 25°C ambient temperature (any color except for red is less than the required 4°/100mm, equivalent to 40°/m as shown in the color scale).

The transient analysis is used to determine the required cooling time to achieve operating temperature. The results show that with an ambient temperature of 300°K, approximately 48 hours (2 days) of cooling time is required to reach the operating temperature of 70°K. This time frame is very consistent for both the optical bench and its subcomponents. The cooling time is reduced to approximately 34 hours (1.4 days) when the ambient temperature is 263°K. The analysis also reveals that the cooling rates (0.30 to 0.34 K/min) are acceptable to prevent thermal shock to optical elements. The temperature versus time curves are shown in Figure 25.

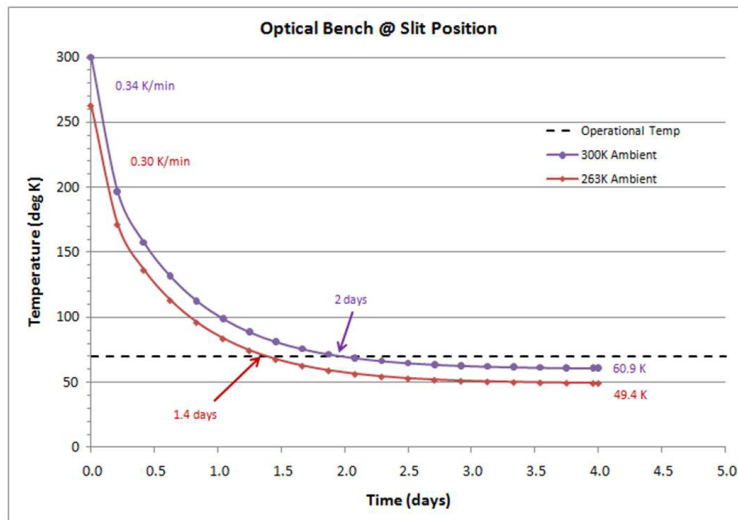


Figure 25. Representative cooling temperature versus time curve for the optical bench at the slit position.

A similar transient analysis was performed to estimate the time required for the cryostat to return to ambient temperature upon shutting the cryocooler refrigerators off. The optical bench and all subcomponents were given an initial temperature of 61°K, which is equal to the average temperature of the optical bench at steady state. The heat power from the cold heads was set to zero and the cold heads were assigned a fixed temperature of 300°K. The remaining types of heat transfer in effect are radiation and conduction from the cold heads. Figure 26 shows the optical bench reached 290°K in 48 hours (2 days) and 298°K in 72 hours (3 days). The maximum warming rate is 0.21 K/min which is also well within limits of preventing thermal shock to optical elements.

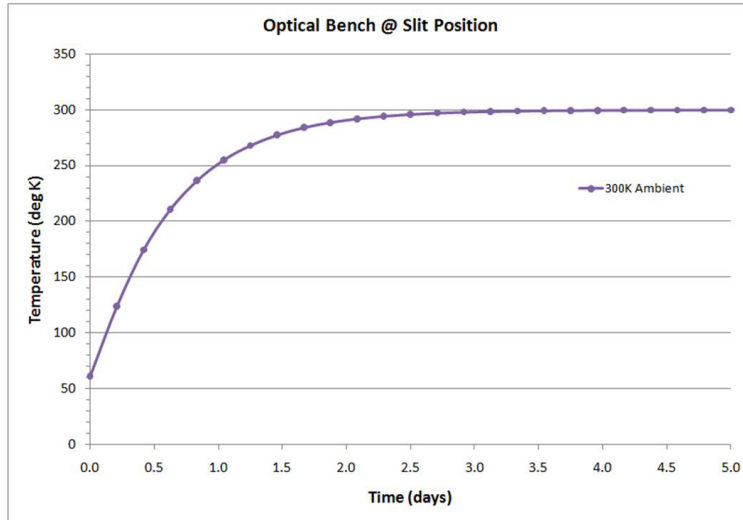


Figure 26. Temperature vs. time curve for the optical bench at the slit position while returning to ambient temperature.

3.5 Mass budget

Table 4 shows the mass values for the subsystems of the GMTNIRS instrument. The entire cryostat, which includes the midsection, top and bottom hatches, and the legs, has a mass of 971 kg. The optical bench, including all three modules, has a mass of 370 kg. The optical hardware mounted to the optical bench has a mass of 214 kg. There is a miscellaneous component included, which should account for the various cryostat fasteners and additional hardware not accounted for in the solid models. The radiation shield assembly, which includes all components forming the upper and lower shields, has a mass of 26 kg. The input window assembly, which includes the lens, retaining ring, etc. has a mass of 14 kg. The thermal isolation system, which includes the four X-brace assemblies, has a total mass of 14 kg. The total system mass is 1639 kg.

Table 4. Estimated mass budget for proposed GMTNIRS instrument.

<u>Component</u>	<u>Mass (kg)</u>	<u>Total (kg)</u>
Cryostat	971	
Optical Bench	370	
Optical Hardware	214	
Miscellaneous	30	
Radiation Shield	26	
Input Window	14	
Thermal Isolation System	14	
		1639

4. CONCLUSIONS

The structural-mechanical design concept of the GMTNIRS instrument satisfies the GMT-specific and science requirements. Analyses, both structural and thermal, confirm that the requirements are met and validate the design points and methodologies chosen. GMTNIRS instrument functionality stands to open significant discovery space, while the relative simplicity of the instrument reduces cost and risk.

5. REFERENCES

- [1] Jaffe, D., "GMTNIRS CoDR Report," Concept design review, submitted to GMT Board Oct. 3, 2011.
- [2] Lee, S., "GMTNIRS (Giant Magellan Telescope Near-Infrared Spectrograph): Design concept," Proc. SPIE 7735, 2010.
- [3] Jaffe, D., "IGRINS preliminary design review," Preliminary design review presented Dec. 3, 2009.
- [4] Jones, D., "GMTNIRS optical component tolerance and sensitivity analysis," Prime Optics, Australia, August 15, 2011.
- [5] Stahlberger, V., "Cryostat Design," Institute for Astronomy, University of Hawaii, 2001.
- [6] Marquardt, E.D., "Cryogenic material database," 11th International Cryocooler Conference, 2000.
- [7] Ravi-Chandar, K., "Mechanical properties of G-10 glass-epoxy composite," Institute for Advanced Technology, The University of Texas at Austin, Technical Report, 2007.
- [8] McLean, I., "Design and development of MOSFIRE, the Multi-Object Spectrometer for Infra-Red Exploration at the Keck Observatory," SPIE Vol. 7735, 2010.
- [9] Stahlberger, V., "Mechanism Library," Institute for Astronomy, University of Hawaii, 2001.